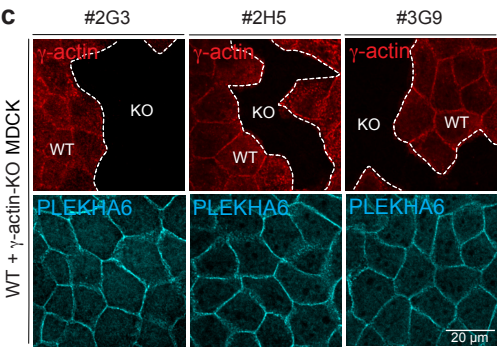
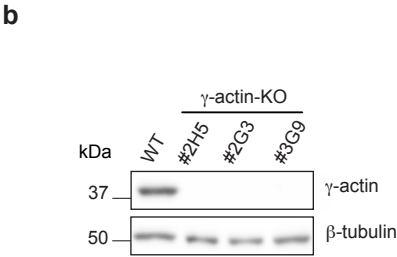
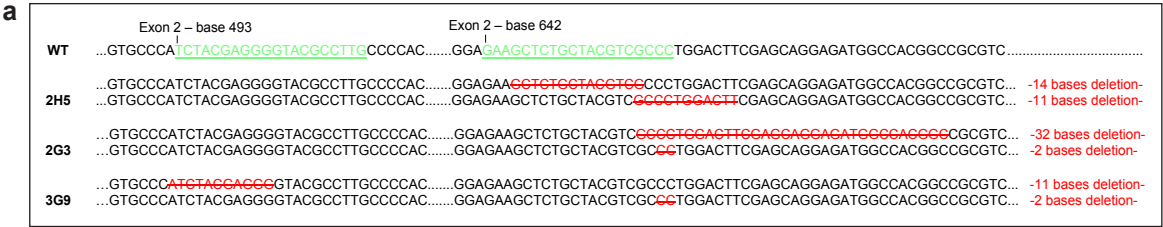


SUPPLEMENTARY INFORMATION

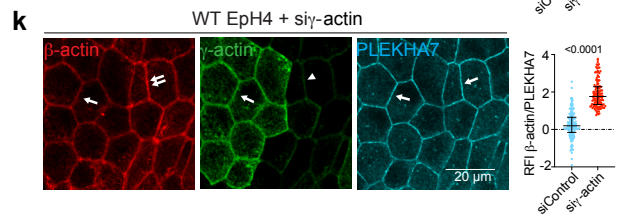
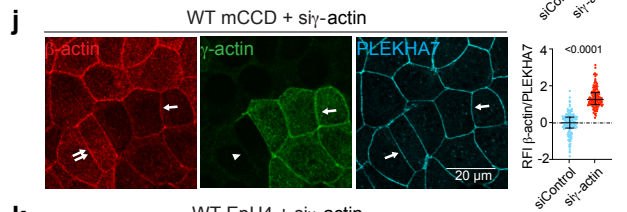
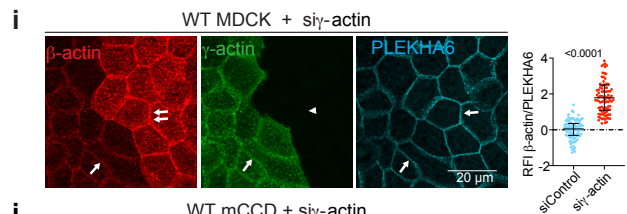
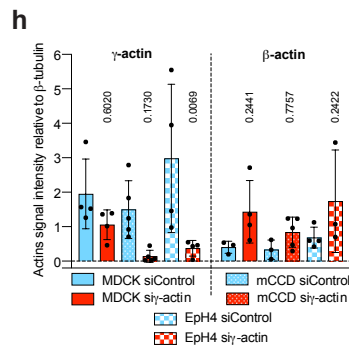
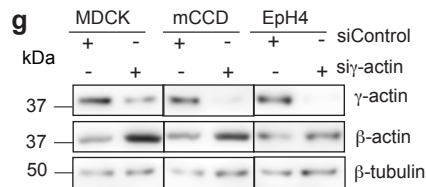
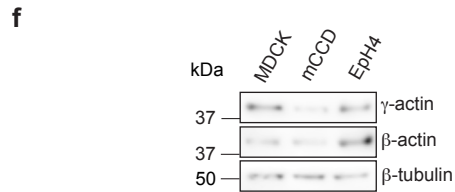
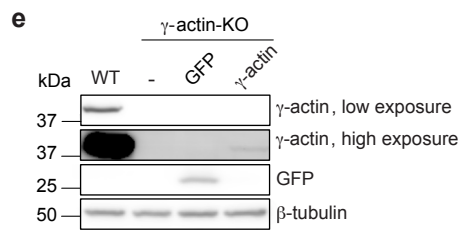
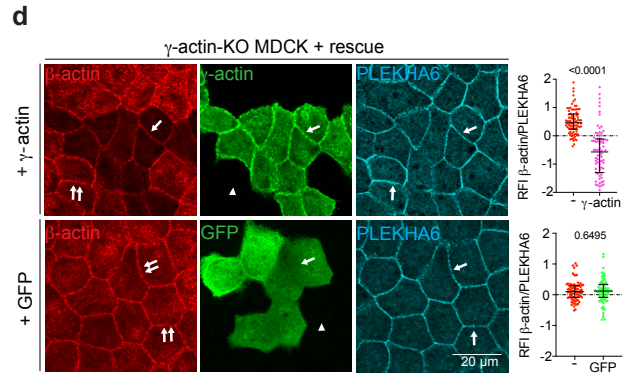
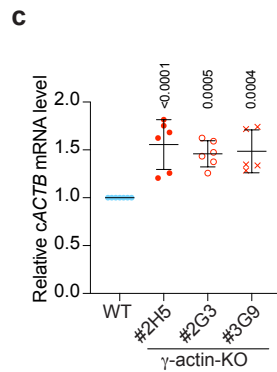
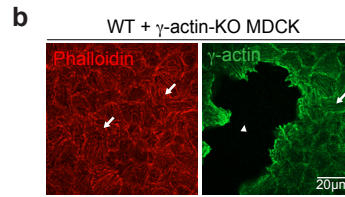
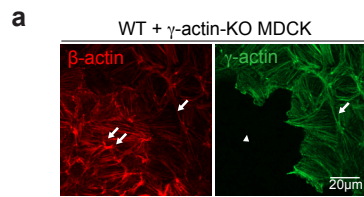
Supplementary Figures



Supplementary Figure 1. Generation of MDCK cells KO for γ -actin using Crispr/Cas9.

(a-c) Validation of Crispr/Cas9-mediated deletion of γ -actin in WT MDCK background by genomic sequencing (a), IB (b) and IF microscopy (c) analysis.

For genomic sequencing, Crispr targets are coloured in green in WT sequence with their position in the exon, base deletions in the alleles of the KO clones obtained are highlighted by strikeout red. For IB analysis, β -tubulin is used as a loading control. For IF microscopy analysis, PLEKHA6 is used as junctional marker reference. Scale bar = 20 μ m.



Supplementary Figure 2. The KO of γ -actin specifically affects the mRNA and protein expression of β -actin in different epithelial cell types.

(a-b) IF microscopy analysis of the localization of either β -actin (a) or phalloidin (b) in the basal region of mixed cultures of WT and γ -actin-KO MDCK.

(c) Relative mRNA levels of *cACTB* (β -actin) normalized by *cHPRT* in WT (blue dots) and γ -actin-KO (red dots) MDCK using RT-qPCR from 6 independent experiments. Dots shows replicates and bars represent mean \pm SD. Indicated p-values are obtained from a two-sided one-way Anova test.

(d) IF microscopy analysis and RFI quantifications of β -actin (red) at junctions in γ -actin-KO (red dots) rescued with either γ -actin (pink dots, top panels, γ -actin-KO: n=85, γ -actin-KO+ γ -actin: n=79), or GFP (green dots, bottom panels, γ -actin-KO: n=80, γ -actin-KO+GFP: n=81) from 3 independent experiments.

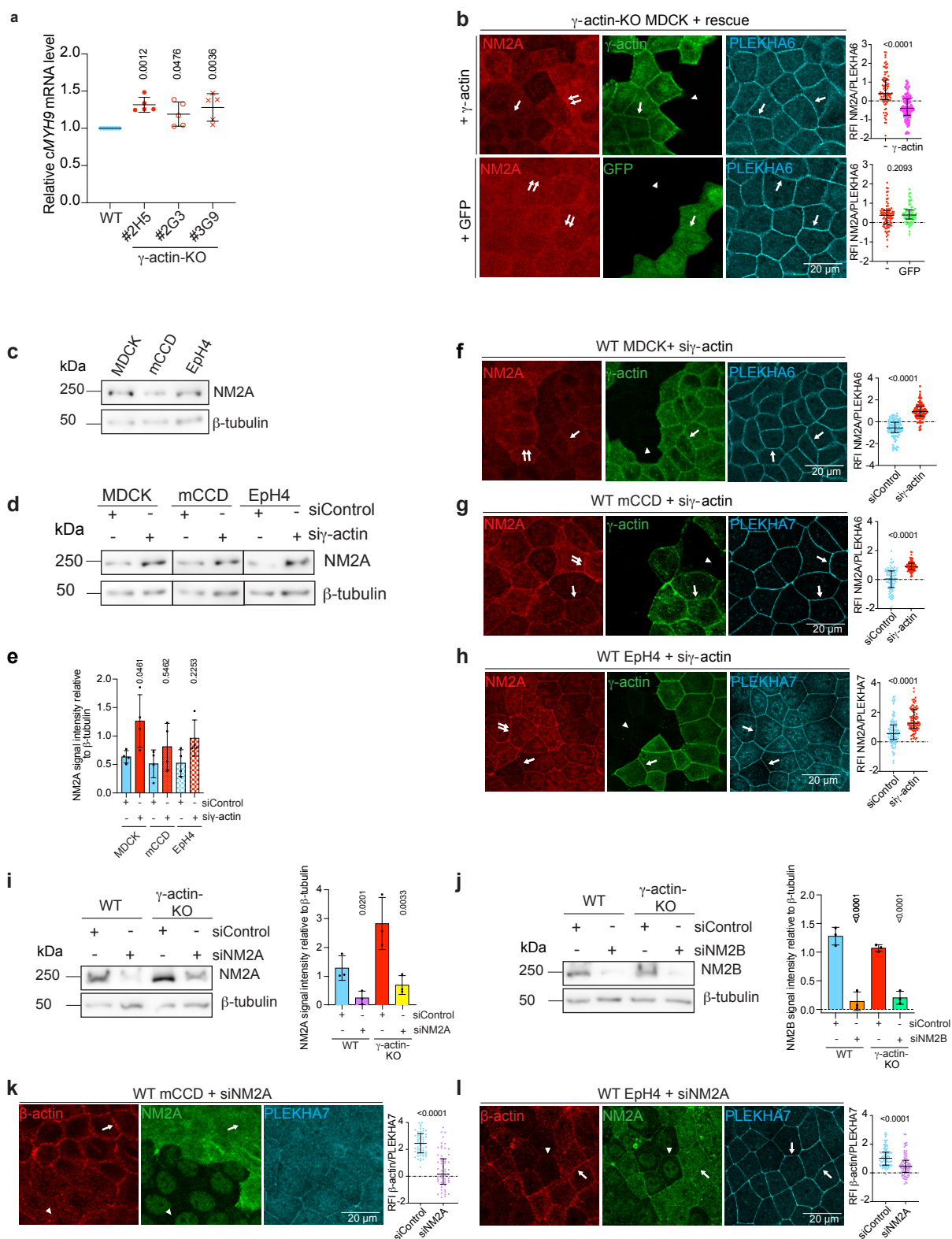
(e) IB analysis of protein level of γ -actin and GFP in lysates of WT, γ -actin-KO, and γ -actin-KO rescued with either γ -actin or GFP. 2 exposure levels were used: low and high.

(f) IB analysis of protein level of γ -actin and β -actin in lysates of WT MDCK, mCCD and EpH4 from 3 independent experiments.

(g-h) IB analysis (g) and relative densitometric quantifications (h) of protein levels of γ -actin and β -actin in lysates of WT MDCK, mCCD and EpH4 treated with siControl (blue dots) or si γ -actin (red dots) from 5 independent experiments. β -tubulin was used as a loading control. Indicated p-values are obtained from a two-sided one-way Anova test.

(i-k) IF microscopy analysis and RFI quantifications of β -actin (red) at junctions in WT (blue dots) MDCK (siControl: n=94, si γ -actin: n=100) (i), mCCD (siControl: n=132, si γ -actin: n=141) (j) or EpH4 (siControl: n=142, si γ -actin: n=137) (k) upon γ -actin depletion (red dots) from 2-3 independent experiments.

(a-b, d, i-k) KO/KD/rescue cells were distinguished from WT γ -actin or GFP (green). Arrows indicate normal labelling (as in WT). Double-arrows indicate increased labelling for β -actin. Arrowheads indicate loss of γ -actin labelling in KO or KD cells. PLEKHA6 or PLEKHA7 are used as junctional markers (cyan). Scale bar = 20 μ m. Dots shows replicates and bars represent mean \pm SD. Indicated p-values are obtained from a two-sided unpaired Mann-Whitney test. Source data for this figure are provided as a Source Data file.



Supplementary Figure 3. The KO of γ -actin specifically affects the mRNA and protein expression of NM2A in different epithelial cell types, and this in turn affects β -actin.

(a) Relative mRNA levels of *cMYH9* (NM2A) normalized by *cHPRT* in WT (blue dots) and γ -actin-KO (red dots) MDCK using RT-qPCR from 5 independent experiments. Dots shows replicates and bars represent mean \pm SD. Indicated p-values are obtained from a two-sided one-way Anova test.

(b) IF microscopy analysis and RFI quantifications of NM2A (red) at junctions in γ -actin-KO (red dots) rescued with either γ -actin (pink dots, top panels, γ -actin-KO: n=89, γ -actin-KO+ γ -actin: n=85), or GFP (green dots, bottom panels, γ -actin-KO: n=82, γ -actin-KO+GFP: n=74) from 3 independent experiments.

(c) IB analysis of protein level of NM2A in lysates of WT MDCK, mCCD and Eph4 from 3 independent experiments.

(d-e) IB analysis (d) and relative densitometric quantifications (e) of protein levels of NM2A in lysates of WT MDCK, mCCD and Eph4 treated with siControl (blue dots) or si γ -actin (red dots) from 4 independent experiments.

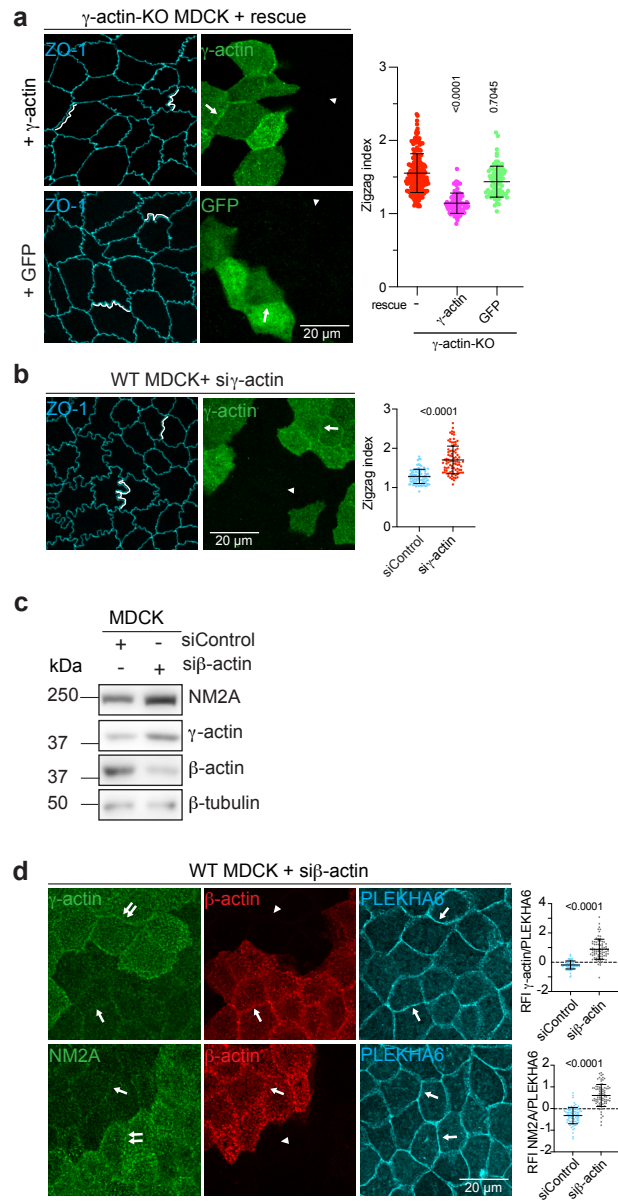
(f-h) IF microscopy analysis and RFI quantifications of NM2A (red) at junctions in WT (blue dots) MDCK (siControl: n=98, si γ -actin: n=95) (f), mCCD (siControl: n=86, si γ -actin: n=97) (g) or Eph4 (siControl: n=105, si γ -actin: n=97) (h) upon γ -actin depletion (red dots) from 2-3 independent experiments.

(i-j) IB analysis and relative densitometric quantifications of protein level of NM2A (i) or NM2B (j) in lysates of WT or γ -actin-KO treated with siControl, siNM2A or siNM2B from 3 independent experiments.

(c-e, i-j) β -tubulin was used as a loading control. Dots shows replicates and bars represent mean \pm SD. Indicated p-values are obtained from a two-sided one-way Anova test.

(k-l) IF microscopy analysis and RFI quantifications of β -actin (red) at junctions in WT (blue dots) mCCD (siControl: n=55, siNM2A: n=60) (k) or Eph4 (siControl: n=88, siNM2A: n=82) (l) upon NM2A depletion (purple dots) from 3 independent experiments.

(b, f-h, k-l) Arrows indicate normal junctional NM2A/ β -actin localization. Double-arrows indicate junctional NM2A enrichment. Arrowheads indicate decreased labelling for γ -actin/NM2A/ β -actin in KO/KD cells. PLEKHA6 or PLEKHA7 are used as junctional markers (cyan). Scale bar = 20 μ m. Dots shows replicates, bars represent mean \pm SD. Indicated p-values are obtained from a two-sided unpaired Mann-Whitney test. Source data for this figure are provided as a Source Data file.



Supplementary Figure 4. The KD of γ -actin results in increased TJ membrane tortuosity and is rescued by exogenous expression of γ -actin.

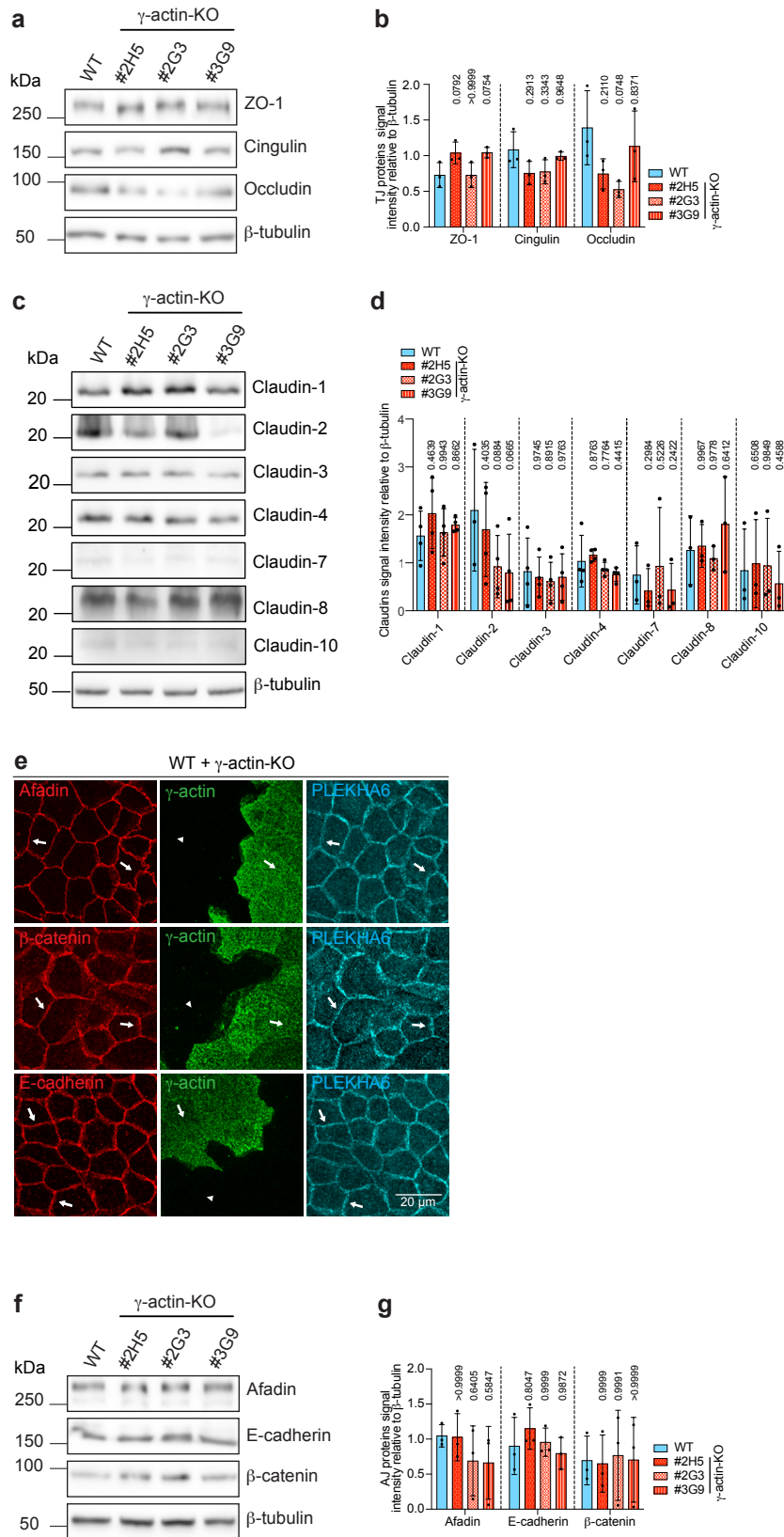
(a) IF microscopy analysis and zigzag index quantifications of ZO-1 (cyan); used as a TJ marker; in γ -actin-KO cells (red dots, n=92) rescued with either γ -actin, (pink dots, top panels, n=87), or by GFP (green dots, bottom panels, n=78) distinguished via γ -actin or GFP (green), from 3 independent experiments.

(b) IF microscopy analysis and zigzag index quantifications of ZO-1 (cyan) in WT (blue dots) MDCK cells upon γ -actin depletion (red dots) (siControl and si γ -actin: n=90), distinguished via γ -actin (green), from 3 independent experiments.

(a-b) White line represents the membrane tortuosity. Scale bar = 20 μ m. Dots shows replicates and bars represent mean \pm SD. Indicated p-values are obtained from a two-sided unpaired Mann-Whitney test.

(c) IB analysis of protein level of NM2A, γ -actin and β -actin in lysates of WT MDCK treated with siControl or si β -actin. β -tubulin was used as a loading control from 3 independent experiments. Dots shows replicates and bars represent mean \pm SD. Indicated p-values are obtained from a two-sided one-way Anova test.

(d) IF microscopy analysis and RFI quantifications of γ -actin (top panel, siControl: n=86, si β -actin: n=78) or NM2A (bottom panel, siControl: n=82, si β -actin: n=84) (green) at junctions in WT MDCK cells (blue dots) upon β -actin depletion (grey dots), distinguished via β -actin (red), from 3 independent experiments. Arrows indicate normal junctional γ -actin and NM2A localization. Double-arrows indicate junctional γ -actin and NM2A enrichment. PLEKHA6 was used as a junctional marker (cyan). Scale bar = 20 μ m. Dots shows replicates and bars represent mean \pm SD. Indicated p-values are obtained from a two-sided unpaired Mann-Whitney test. Source data for this figure are provided as a Source Data file.



Supplementary Figure 5. The KO of γ -actin does not perturb the expression of TJ, AJ and claudin proteins, and the junctional accumulation of AJ proteins in MDCK cells.

(a-d) IB analysis (a, c) and relative densitometric quantifications (b, d) of protein level of either TJ (ZO-1, cingulin and occludin, not changed) (a-b), or claudin (claudin-1, -2, -3, -4, -7, -8, -10, not changed) (c-d) proteins in lysates of WT (blue dots) and γ -actin-KO (red dots, 3 distinct clonal lines) MDCK cells from 3-4 independent experiments.

(e) IF microscopy analysis of endogenous afadin, E-cadherin and β -catenin (AJ proteins, red, not changed) in mixed cultures of WT (blue dots) and γ -actin-KO (red dots) cells, distinguished via γ -actin (green), from 2-3 independent experiments. PLEKHA6 (cyan) is used as a junctional marker. Scale bar = 20 μ m.

(f-g) IB analysis (f) and relative densitometric quantifications (g) of protein level of afadin, E-cadherin and β -catenin (not changed) in lysates of WT (blue dots) and γ -actin-KO (red dots, 3 distinct clonal lines) MDCK cells from 3 independent experiments.

(a-d, f-g) β -tubulin was used as a loading control. Dots shows replicates and bars represent mean \pm SD. Indicated p-values are obtained from a two-sided one-way Anova test. Source data for this figure are provided as a Source Data file.

Supplementary Table 1. Resources table

Reagent of resources	Source / Reference	Identifier
Antibodies		
Mouse IgG2b monoclonal anti- γ -actin (IB, IF)	Prof. C. Chaponnier, University of Geneva ¹	2A368E2 RRID:AB_2571583
Mouse IgG1 monoclonal anti- β -actin (IB, IF)	Prof. C. Chaponnier, University of Geneva ¹	4C259H12 RRID:AB_2571580
Rat polyclonal anti-PLEKHA6 (IF)	²	RtSZR127
Guinea pig polyclonal anti-PLEKHA7 (IF)	²	GP2737
Rabbit polyclonal anti-NM2A (IB, IF)	Biolegend	Cat# 909801 RRID:AB_291638
Rabbit polyclonal anti-NM2B (IB, IF)	Biolegend	Cat# 909901 RRID:AB_291639
Mouse monoclonal anti-pan-actin (IB)	Sigma-Aldrich/Merck	Cat# mab1501 RRID: AB_2223041
FITC-phalloidin (IF)	Sigma	Cat# P5282
Alexa Fluor™ 488 Phalloidin	Invitrogen™	Cat# A12379
Mouse monoclonal anti-GFP (IF)	Roche	Cat# 11814460001, RRID:AB_390913
Mouse monoclonal anti- β -tubulin (IB)	Thermo Scientific	Cat# 32-2600 RRID: AB_2533072
Rat monoclonal anti-ZO-1 (IF)	Prof. Daniel Goodenough, Harvard Medical School	R40.76, RRID:AB_2205518
Mouse monoclonal anti-ZO-1 (IB)	Thermo Scientific	Cat# 3391000 RRID: AB_2533147
Rabbit polyclonal anti-cingulin (IB, IF)	Citilab	C532
Rabbit polyclonal anti- β -catenin (IB, IF)	Sigma-Aldrich/Merck	Cat# C2206 RRID: AB_326078
Rabbit polyclonal anti-E-cadherin	Santa Cruz	Cat# 7870 RRID: AB_2076666
Mouse monoclonal anti-E-cadherin	BD Biosciences	Cat# BD 610181 RRID:AB_397580
Rabbit polyclonal anti-Claudin-1 (IB)	Thermo Scientific	Cat# 51-9000 RRID: AB_2533916
Mouse monoclonal anti-Claudin-2 (IB)	Thermo Scientific	Cat# 32-5600 RRID: AB_2533085
Rabbit polyclonal anti-Claudin-3 (IB)	Thermo Scientific	Cat# 34-1700 RRID: AB_2533158
Mouse monoclonal anti-Claudin-4 (IB)	Thermo Scientific	Cat# 32-9400

		RRID: AB_2533096
Rabbit polyclonal anti-Claudin-7 (IB)	Thermo Scientific	Cat# 34-9100 RRID: AB_2533190
Rabbit polyclonal anti-Claudin-8 (IB)	Thermo Scientific	Cat# 40-0700Z RRID: AB_2533445
Rabbit polyclonal anti-Claudin-10 (IB)	Thermo Scientific	Cat# 38-8400 RRID: AB_2533386
Cy3-AffiniPure Donkey anti-Mouse IgG	Jackson Laboratory	Cat# 715-165-151 RRID: AB_2315777
Cy3-AffiniPure Donkey anti-Rat IgG	Jackson Laboratory	Cat# 712-166-150 RRID: AB_2340668
Alexa Fluor 488-AffiniPure Donkey anti-Rabbit IgG	Jackson Laboratory	Cat# 711-545-152 RRID: AB_2313584
Cy5-AffiniPure Donkey anti-Rat IgG	Jackson Laboratory	Cat# 712-175-153 RRID: AB_2340672
Cy5-AffiniPure Donkey anti-Mouse IgG	Jackson Laboratory	Cat# 715-175-150 RRID: AB_2340819
Anti-mouse IgG (H+L), HRP Conjugate	Promega	Cat# W4021 RRID: AB_430834
Anti-rabbit IgG (H+L), HRP Conjugate	Promega	Cat# W4011 RRID: AB_430833
Plasmids		
pTRE2Hyg-GFP-myc	3	S1210
pTRE2Hyg-GFP-cingulin-FL-myc	4	S1052
pTRE2Hyg-GFP-ZO-1-FL	5	S2474
pTRE2Hyg-ACTG1-FL	This paper	S2882
pTRE2Hyg-ACTB-FL	This paper	S2926
Chemicals, Reagents, Peptides, Critical commercial assays		
Pierce Protease Inhibitor Tablet, EDTA-free	Thermo Scientific	Cat# A32965
jetOPTIMUS	Polyplus	Cat# 117-15
Lipofectamine RNAiMAX	Invitrogen	Cat# 13778030
Hanks buffer	Gibco	Cat# 14025-050
3 kDa fluorescein-dextran	Invitrogen	Cat# D3305
OptiMeM	Gibco	Cat# 51985-026
DMEM without phenol red	Gibco	Cat# 21063-029
NucleoSpin® RNA kit	Macherey-Nagel	Cat# 740955.50
iScript™ cDNA Synthesis kit	Bio-Rad	Cat# 1708890
Master Mix Select SYBR™ kit	Thermo Scientific	Cat# 4472908
Pierce BCA Protein assay kit	Thermo Scientific	Cat# 23225

WesternBright ECL kit	Advansta	Cat# K-12045-D50
Molecular Weight Markers for SDS-PAGE	BioRad	Cat# 1610373
DNeasy Blood and Tissue kit	Qiagen	Cat# 69504
Hoechst	Thermo Scientific	Cat# 33342
Blebbistatin	Sigma-Aldrich/Merck	Cat# B0560
Bovines Serumalbumin (BSA)	Carl Roth GmbH	Cat# 3737.1
Dulbecco's Phosphate Buffered Saline (PBS)	Gibco™	Cat# 21600-051
Glass coverslips 1.5H 22 x 22 mm	Carl Roth GmbH	Cat# KCY1.1
Microscope slides, corners grounded 90°, without frosted edge	Carl Roth GmbH	Cat# H869.1
Mowiol® 4-88	Carl Roth GmbH	Cat# 0713.2
Paraformaldehyde (PFA)	Science Services	Cat# E15714
Poly-D-Lysine Hydrobromide	Sigma-Aldrich	Cat# P7405-5MG
6-well tissue culture plate, flat bottom, polystyrene	TPP Techno Plastic Products AG	Cat# 92406
Experimental models: Cell lines		
Madin-Darby Canine Kidney Tet-Off (MDCK) WT	A. Fanning, University of North Carolina	Clontech
Madin-Darby Canine Kidney Tet-Off (MDCK) γ -actin-KO	This paper	N/A
Mouse mammary epithelial cell line (Eph4) WT	Reichmann Laboratory, ⁶	N/A
Mouse Cortical Collecting Duct Cell Line (mCCD) WT	Férraille Laboratory, University of Geneva ⁷	N/A
Oligonucleotides		
siRNA targeting sequence : canis γ -actin GUUAACUGUCCCUUGGUAUA	This paper	Microsynth
siRNA targeting sequence : canis β -actin AAACCUAACUUGCGCAGAA	This paper	Microsynth
siRNA targeting sequence : canis NM2A GAAGAUCACAGACGUCAUUAU	This paper	Microsynth
siRNA targeting sequence : canis NM2B GCUACUAUUCGGGAUUGAUCU	This paper	Microsynth
siRNA negative control: CGUACGCGGAUACUUCGA	This paper	Microsynth
CRISPR target sequence: canis <i>ACTG1</i> TCTACGAGGGGTACGCCTTG	This paper	Genscript
CRISPR target sequence: canis <i>ACTG1</i> GAAGCTCTGCTACGTCGCCC	This paper	Genscript

RT-qPCR target sequence: canis <i>ACTB</i> Fw: AGCGCAAGTACTCTGTGTGG Rv: GTAACAGTCCGCCTAGAAGC	This paper	Microsynth
RT-qPCR target sequence: canis <i>MYH9</i> Fw: CTGCAAAGTGGCCAAGGAGA Rv: GTCGGTGATCATCGCCTCAT	This paper	Microsynth
RT-qPCR target sequence: canis <i>HPRT</i> Fw: TGGACAGGACTGAGCGGC Rv: TGAGCACACAGAGGGCTACG	This paper	Microsynth
Software and algorithms		
Image J	N/A	Imagej.nih.gov/ij/ RRID: SCR_003070
Affinity Designer	N/A	https://affinity.serif.com/ RRID: SCR_016952
Prism GraphPad	N/A	https://www.graphpad.com/scientific-software/prism/ RRID: SCR_002798
Snapgene Version 3.1.2	N/A	snapgene.com RRID:SCR_015052

References for Supplementary Table 1

1. Dugina V, Zwaenepoel I, Gabbiani G, Clement S, Chaponnier C. Beta and gamma-cytoplasmic actins display distinct distribution and functional diversity. *J Cell Sci* **122**, 2980-2988 (2009).
2. Sluysmans S, *et al.* PLEKHA5, PLEKHA6 and PLEKHA7 bind to PDZD11 to target the Menkes ATPase ATP7A to the cell periphery and regulate copper homeostasis. *Mol Biol Cell* **32**, 1-20 (2021).
3. Zheng CY, Petralia RS, Wang YX, Kachar B. Fluorescence recovery after photobleaching (FRAP) of fluorescence tagged proteins in dendritic spines of cultured hippocampal neurons. *J Vis Exp*, (2011).
4. D'Atri F, Citi S. Cingulin interacts with F-actin in vitro. *FEBS Lett* **507**, 21-24 (2001).
5. Mauperin M, Sassi A, Mean I, Feraille E, Citi S. Knock Out of CGN and CGNL1 in MDCK Cells Affects Claudin-2 but Has a Minor Impact on Tight Junction Barrier Function. *Cells* **12**, (2023).
6. Fialka I, Schwarz H, Reichmann E, Oft M, Busslinger M, Beug H. The estrogen-dependent c-JunER protein causes a reversible loss of mammary epithelial cell polarity involving a destabilization of adherens junctions. *J Cell Biol* **132**, 1115-1132 (1996).
7. Wang YB, *et al.* Sodium transport is modulated by p38 kinase-dependent cross-talk between ENaC and Na,K-ATPase in collecting duct principal cells. *J Am Soc Nephrol* **25**, 250-259 (2014).

Supplementary notes

Abbreviations

AJC, apical junctional complex; KO, knock-out; FRAP, fluorescence recovery after photobleaching; TJ, tight junction; AJ, adherens junction; NM2, non-muscle myosin-2; KD, knock-down; IB, immunoblot; IF, immunofluorescence; pMLC2, phosphorylated myosin light chain 2; TER, transepithelial resistance; AFM, atomic force microscopy; FSC-A, forward scatter area; MLCK, myosin light chain kinase; ABR, actin binding region; Madin-Darby Canine Kidney-II, MDCK; mCCD, mouse cortical collecting duct; EpH4, mouse mammary; DMEM, Dulbecco's Modified Eagle's; FBS, Fetal Bovine Serum; NEAA, non-essential amino-acids; P/S, penicillin and streptomycin; gRNA, guide RNA; GFP, green fluorescent protein; RT, room temperature; NaCl, sodium chloride; RIPA, radioimmunoprecipitation assay buffer; EDTA, ethylenediaminetetraacetic acid; SDS, sodium dodecyl sulfate; O₂, oxygen; CO₂, carbon dioxide; FC, fold change; FDR, false discovery rate; PIC, protease inhibitor cocktail; PFA, paraformaldehyde; BSA, bovine serum albumin; DAPI, 4',6 diamidino 2 phenylindole; FL, full-length; HBSS, Hank's balanced salt solution; GLM, general linear model; hr, hour; s, seconds; Perm_{app}, apparent permeability; PBS, phosphate buffered saline; DPBS, Dulbecco's phosphate buffered saline; S-MEM, suspension-minimum essential medium; EGF, epidermal growth factor; PLEKHA6, Pleckstrin Homology Domain-Containing, family A member 6; kDa, kilodaltons; ECL, enhanced chemiluminescence; SD, standard deviation; Px, pixels; RFI, relative fluorescence intensity; ns, not significant; WT, wild-type.